Protein atlas of fibroblast specific protein 1 (FSP1)/S100A4

Bettina Marturet Fendt
Institute of Pathology, Cantonal Hospital Lucern
Astrid Hirschmann
Institute of Pathology, Cantonal Hospital Lucern
Malgorzata Bruns
Institute of Pathology, Cantonal Hospital Lucern
Eva Camarillo-Retamosa
Department of Rheumatology, Center of Experimental Rheumatology, University Hospital Zurich
Caroline Ospelt
Department of Rheumatology, Center of Experimental Rheumatology, University Hospital Zurich
Alexander Vogetseder (alexander.vogetseder@luks.ch)
Institute of Pathology, Cantonal Hospital Lucern

Research Article

Keywords: FSP1, S100A4, EMT, protein atlas

Posted Date: April 26th, 2022

DOI: https://doi.org/10.21203/rs.3.rs-1579878/v1

Abstract

Fibroblast specific protein 1 (FSP1/S100A4) is an intracellular calcium binding protein which has been linked to epithelial-mesenchymal transition, tissue fibrosis, pulmonary vascular disease, metastatic tumour development, increased tumour cell motility and invasiveness. This protein is reported to be uniquely expressed in newly formed and differentiated fibroblasts and has been used in various studies to demonstrate epithelial-mesenchymal transition (EMT). However, S100A4 immunoreactivity does not solely fit the distribution and shape of fibroblasts; therefore, we aimed to characterize S100A4 positive cells in different human tissue compartments.

We found S100A4 expression in a wide range of cells, including cells of haematopoietic lineage, namely CD4 and CD8 positive T-lymphocytes, but not B-lymphocytes. All investigated monocytes, macrophages and specialised histiocytes were positive for S100A4. Only a limited number of fibroblasts and most smooth muscle actin positive myofibroblasts expressed S100A4. Even some epithelial cells of the kidney and bladder were positive for S100A4. Expression was also found in the vasculature. Here, cells of the subendothelial space, tunica adventitia and some smooth muscle cells of the tunica media were positive for S100A4. Expression was also detected in the stroma of the prostate, adipocytes and in skeletal muscle.

In summary, S100A4 is expressed in various cell types of different lineage. It is therefore not possible to equate the expression of this protein to fibroblasts. Hence, studies that used this marker as evidence of transition from epithelia to fibroblasts must be revisited.

Introduction

Fibroblast specific protein (FSP1/S100A4) is an intracellular calcium binding protein localized in the cytoplasm and/or nucleus that regulates several cellular processes such as cell cycle progression (Sherbet and Lakshmi 1998) and differentiation as well as motility (Fei et al. 2017) and tubulin polymerization. Additionally, S100A4 is reported to be linked to increased tumour cell motility, invasiveness and metastatic tumour development (Sherbet 2009). This protein, as the name implies, is thought to be solely expressed in fibroblasts/myofibroblasts and its appearance was linked to epithelial-mesenchymal transition (EMT). EMT is the phenotypic transition of epithelial cells to mesenchymal lineage with cells losing their epithelial characteristics and acquiring mesenchymal features. EMT is subdivided into 3 subtypes (Kalluri and Weinberg 2009).

Type 1 EMT is associated with implantation and embryonic gastrulation and gives rise to mesoderm and endoderm as well as mobile neural crest cells. The primitive epithelium, specifically the epiblast, gives rise to primary mesenchyme via EMT. This primary mesenchyme can be reinduced to form secondary epithelia by mesenchymal-epithelial transition (MET). It is speculated that such secondary epithelia may further differentiate to form other types of epithelial tissues, undergoing subsequent EMT to generate the

cells of connective tissue, including astrocytes, adipocytes, chondrocytes, osteoblasts, and muscle cells (Kalluri and Weinberg 2009; Thiery et al. 2009).

Type 3 EMT represents an important stage of the evolution of epithelial cancers that leads to a more aggressive phenotype associated with uncontrolled growth, migration and invasion (sarcomatous growth) (Saitoh 2018).

Type 2 EMT refers to the transition of specialised secondary epithelial cells (e.g., proximal tubular cells in the kidney) into myofibroblasts with substantial pro-fibrotic and pro-inflammatory activity. Proposed steps in type 2 EMT are the loss of cell–cell contact and apical–basal polarity besides cellular destabilisation with reduction of E-cadherin and zonula occludens. In the intermediate phase, both epithelial and mesenchymal markers are expressed, matrix metalloproteinases (especially MMP2 and MMP9) are up regulated and MMP-inhibitors are down regulated, leading to disruption of underlying basement membranes. Finally, there is a transition to mesenchymal phenotype with the formation of the enlarged spindle-shaped myofibroblast (Burns and Thomas 2010).

The first study with the FSP1/S100A4 antibody was published in 1995 (Strutz et al. 1995) and laid the foundation for the hypothesis of type 2 EMT. Based on their investigations using subtractive and differential hybridization for transcript comparison between murine fibroblasts and isogenic epithelium, the authors reported that FSP1 is relatively specific for fibroblasts. Using a mouse model of renal interstitial fibrosis with persistent interstitial inflammation, they hypothesized that fibroblasts in some cases arise from kidney epithelium. Additionally, the in vitro overexpression of FSP1 cDNA in tubular epithelium was accompanied by conversion to a mesenchymal phenotype. Finally, results of experiments with a tubular mouse epithelium cell line submerged in type I collagen gels, lead to the generation of the type 2 EMT hypothesis.

In subsequent years, this hypothesis was tested by employing antibodies directed against FSP1 in other organs such as the liver. These results indicated that adult mouse hepatocytes undergo phenotypic and functional changes typical of epithelial to mesenchymal transition. Additionally, it was reported that hepatocytes, which undergo EMT, contribute substantially to the population of FSP1-positive fibroblasts in liver fibrosis (Zeisberg et al. 2007).

In recent years, the specificity of FSP1/S100A for fibroblasts has been questioned. Since the EMT type 2 theory is based on cells expressing S100A4 (Strutz et al. 1995), we set out to characterise and catalogue cells that express S100A4 in different human tissues.

Material And Methods

Tissue:

Non-malignant paraffin-embedded human tissue samples were retrieved from the pathology archive of the Lucerne cantonal hospital. Sections of 2µm thickness were prepared from soft tissues of different

locations and various organs.

Immunohistochemistry/-fluorescence:

Immunohistochemical staining was performed on a Leica BOND-III Fully Automated IHC & ISH

Staining System (Leica Biosystems), using the Polymer Refine Detection Kit (Leica DS9800) with the following antibodies:

CD3 (Agilent Technologies; A045201), dilution 1:200.

CD4 (Novocastra; NCL-L-CD4-368), dilution 1:200.

CD8 (BioSB ; BSB5173), dilution 1:300.

CD14 (Abcam; 1H5D8) dilution 1:500.

CD45 (Cell Marque; 145M95), dilution 1:400.

CD68 (Agilent Technologies ; M087601), dilution 1:200.

MART-1/Tyrosinase (BioCare medical; CM 178 A), dilution 1:300.

S100 (Agilent Technologies; Z031129), dilution 1:2000.

FSP1/S100A4 (Sigma; HPA007973), dilution 1:2000.

Smooth muscle actin (Cell Marque; 202M-95), dilution 1:300.

For Immunofluorescence, binding sites of the primary antibodies were revealed with Cy3-conjugated goat-anti-rabbit IgG (red) and fluorescein isothyocyanate (FITC)-conjugated goat-anti-mouse IgG (Jackson ImmunoResearch Laboratories, West Grove, PA), respectively. For nuclear staining, 4',6-diamidino-2-phenylindole (DAPI; Sigma) was added. Fluorescent-labeled specimens were examined using a confocal laser scanning microscope (CLSM SP2, Leica, Mannheim, Germany) or a Polyvar microscope (Reichert Jung, Vienna, Austria).

Cell culture:

Synovial tissues were obtained from rheumatoid arthritis (RA) patients undergoing joint replacement surgery at the Schulthess Clinic Zurich, Switzerland. RA patients fulfilled the 2010 ACR/EULAR (American College of Rheumatology/European League Against Rheumatism) criteria for the classification of RA. The study was approved by the local ethic committees of the University Hospital Zurich, Switzerland. Informed consent was obtained from all patients. Synovial tissues were digested with dispase (37°C, 1 h) and synovial fibroblasts were cultured in Dulbecco's modified Eagle's medium (DMEM; Life Technologies) supplemented with 10% fetal calf serum (FCS), 50 U ml − 1 penicillin/streptomycin, 2 mM L-glutamine, 10

mM HEPES and 0.2% amphotericin B (all from Life Technologies). Synovial fibroblasts from passages 5 to 8 were used.

3D micromasses were generated as previously described(Kiener et al. 2010). In brief, synovial fibroblasts were mixed with Matrigel (LDEV-free, Corning) ($3x10^6$ SF/ml Matrigel) and 30 µl droplets added to 12-well plates coated with poly 2-hydroxyethylmethacrylate (Sigma). Micromasses were left in culture for 3 weeks in Dulbecco's modified Eagle's medium (DMEM; Life Technologies) supplemented with 10% fetal calf serum (FCS), 1% penicillin/streptomycin, 1% minimum Essential medium non-Essential Amino Acids (Gibco), 1% ITS + premix (BD) und 8.8 mg/500 ml vitamin C. After 3 weeks, micromasses were fixed with 2% paraformaldehyde. After 24 h paraformaldehyde was replaced by 70% ethanol and micromasses were embedded in paraffin and sectioned for IHC.

Isolation of peripheral blood mononuclear cells (PBMCs):

EDTA blood was withdrawn from a healthy volunteer. 30ml blood was overlaid over 15 ml Ficoll Paque plus at room temperature. The sample was centrifuged for 30 minutes at 450g without breaks. Mononuclear cells from the interface were collected and suspended in PBS. After three additional washing and centrifugation steps, cells are resuspended in an appropriate medium and spun down on histological slides.

Investigated tissues:

PBMCs were isolated from peripheral blood and co-stained with S100A4 and different leukocyte markers (CD3, CD4, CD8 and CD14) to exclude a relevant contamination with fibroblasts. CD3 was used as pan-T cell marker, CD4 to identify T-helper cells and CD8 for cytotoxic T-cells. CD14 was used as marker for monocytes.

Human lymph node was incubated with CD68, CD3 and S100A4. CD68 was used to identify tissue macrophages.

Human kidney, gallbladder, pancreas, oesophagus, colon, stomach, small intestine, liver, thyroid gland, breast, skin, adrenal gland, urinary bladder, prostate, ovary, uterus, skeletal muscle, brain and testis were stained with S100A4 and analysed.

Human skin was additionally stained with CD68 and MART-1 (melanocyte marker).

Connective tissue was incubated with S100A4 and the structures that make up the connective tissue were analysed for S100A4 positivity. These structures included the vasculature, nerve tissue, adipocytes, inflammatory cells and mesenchymal cell of the connective tissue. To investigate tissue rich in fibroblasts and myofibroblasts, we used hypertrophic scar tissue of the skin and palmar fibromatosis. Additionally, human synovial fibroblast cultures (2D and 3D), attained from joints of rheumatoid arthritis patients were stained with S100A4 and smooth muscle actin. Also, fibroblast rich tendon was stained with S100A4.

Results

In PBMCs, S100A4 was expressed in most CD3 + lymphocytes (Fig. 1a). The analysis showed S100A4 expression in CD4 (Fig. 1b) as well as CD8 positive T-lymphocytes (Fig. 1c). In these cells, S100A4 staining was predominantly cytoplasmic. Also, CD14 + monocytes stained positive for S100A4 (Fig. 1d), displaying a nuclear and cytoplasmic positivity.

In lymph nodes (Fig. 2a), S100A4 staining was observed in areas rich in T cells (Fig. 2c) and in CD68 + histiocytes and dendritic cells (Fig. 2b, d) but not in B cell rich areas (Fig. 2d). In vessels of connective tissue (Fig. 3a, b), S100A4 was highly expressed (nuclear and cytoplasmic) in cells of the subendothelial space, consisting of intimal smooth muscle cells, stellate-shaped pericyte-like cells and in the loose connective tissue of the tunica adventitia. Some positive cells were seen in the tunica media composed of smooth muscle cells, which expressed S100A4 in the cytoplasm. S100A4 was also expressed in the nuclei of most adipocytes of connective tissue (Fig. 3c, d). S100A4 was not detectable in peripheral nerves (Fig. 3c, d), unlike other S-100 antibodies directed against different alpha and beta subtypes(Gonzalez-Martinez et al. 2003). Muscle fibres of skeletal muscle showed staining for S100A4 (Fig. 3e). Less intense and more localised was the S100A4 expression of smooth muscle cells in the urothelial mucosa (Fig. 3f). Also, the urothelium showed cytoplasmic positivity in occasional umbrella cells (Fig. 3f).

In skin (Fig. 4a), S100A4 staining was negative in keratinocytes, but showed strong positive staining in Langerhans cells (Fig. 4b, d). Melanocytes did not express S100A4 (Fig. 4c).

In hypertrophic scar tissue (Fig. 5a), S100A4 showed variable cytoplasmic expression in dermal fibroblasts (Fig. 5d), often stronger in cells co-expressing smooth muscle actin (myofibroblasts; Fig. 5c). S100A4 staining was also seen in CD45 + leukocytes in this tissue (Fig. 5b). Stronger expression of S100A4 was seen in superficial fibromatosis (Fig. 6a, c, d). Also, here S100A4 expression mostly overlapped cells staining positive for smooth muscle actin (Fig. 6b).

Cultured synovial fibroblasts were predominantly negative for S100A4 (Fig. 7a). Smooth muscle actin was rarely expressed by these fibroblasts (Fig. 7b). Accordingly, positive immunohistochemical signal for S100A4 was only clearly detectable in the outer perimeter of 3D cultures of synovial fibroblasts (Fig. 7b), without staining for smooth muscle actin (Fig. 7d). Similarly, fibroblasts of tendon did mostly not or only weakly express S100A4 (Fig. 7e, f).

In the kidney (Fig. 8a, c), S100A4 was expressed in epithelial structures. The strongest and most uniform expression (nuclear and cytoplasmic) was seen in the loop of Henle (Fig. 8b). Also, many cells in the collecting duct expressed S100A4 (Fig. 8b). The distal tubules showed some nuclear and cytoplasmic positivity, more pronounced in the cortex of the kidney (Fig. 8d), with the most homogenous positivity seen in the macula densa (Fig. 8d).

Other investigated organs, including liver, breast, thyroid gland, pancreas, gallbladder, oesophagus, stomach, small intestine, skin and colon, did not express S100A4 in the epithelium (data not shown). The myofibroblast rich stromal cells of the prostate showed a diffuse predominantly moderate cytoplasmic expression of S100A4 (data not shown). The epithelial component in the prostate was negative for S100A4. Only a minority of cells of the uterine myometrium, made up of smooth muscle, showed a weak to moderate cytoplasmic expression of S100A4, the epithelium showed no reactivity for S100A4 (data not shown). The germinal epithelium of testis was negative for S100A4 (data not shown). The hormone secreting cells of the adrenal cortex were negative for S100A4, whereas the surrounding sustentacular cells were positive for S100A4 (nuclear and cytoplasmic).

Astrocytes and oligodendrocytes in brain tissue did not express S100A4, but microglia were positive (data not shown).

In general, the strongest and most consistent nuclear and cytoplasmic S100A4 expression levels were seen in monocytes (Fig. 1d), macrophages and specialised histiocytes, including dendritic cells in lymph nodes (Fig. 2b, d), Langerhans cells of the skin (Fig. 4b, d), Kupffer cells of the liver (data not shown) and microglia of the brain (data not shown).

Discussion

To survey the distribution and extent of the expression of the calcium-binding protein S100A4, we evaluated a broad range of organs and connective tissue incubated with a commonly used FSP1/S100A4 antibody. We found that S100A4 is expressed in wide range of cells, including cells of hematopoietic linage, connective tissue, including fibroblasts/myofibroblasts and even some epithelial cells of the kidney and bladder. The FSP1/S100A4 antibody is therefore not specific for fibroblasts. In many instances, FSP1/S100A4 was hardly detectable in fibroblasts in certain locations like tendon and synovium. In other locations, S100A4 was detectable in fibroblasts/myofibroblasts, especially in tissue with a high portion of smooth muscle actin positive myofibroblasts. Also, other cells found in connective tissue expressed S100A4. Most adipocytes and various compartments of the vasculature such as cells of the subendothelial space and adventitia were positive for S100A4.

We could show that colocalization of S100A4 and smooth muscle actin was especially prominent in myofibroblast rich tissue, where cytoplasmic positivity was discernible in many cells. This co-localization might be linked to motility, a central function of S100A4, as was shown for histiocytic motility (Li et al. 2010). In contrast, S100A4 was hardly detectable in fibroblast rich compartments with a limited expression of smooth muscle actin, including tendon and synovial fibroblasts. Proteomic and localization studies have shown that S100A4 is enriched in the pseudopodia of migrating cells (Kim and Helfman 2003; Li and Bresnick 2006; Wang et al. 2007). Moreover, a S100A4 biosensor, which reports on Ca^{2+}-bound S100A4, has shown that activated S100A4 localizes to the leading edge of polarized, migrating cells (Garrett et al. 2008). The enrichment of S100A4 in protrusive structures is consistent with cell-based functional studies demonstrating that S100A4 expression modulates the migratory capacities of a broad

range of cell types (Jenkinson et al. 2004; Li and Bresnick 2006; Li et al. 2010). Consistent with a role in regulating cell motility, S100A4 has a number of reported cytoskeletal and scaffold protein targets including non-muscle tropomyosin 2, liprin-β1 and non-muscle myosin-IIA (Takenaga et al. 1994; Kriajevska et al. 2002; Kriajevska et al. 1994; Ramagopal et al. 2013). Non-myosin IIA is a key cytoskeletal motor converting the chemical energy of adenosine triphosphate (ATP) into mechanical forces that mediate a static tension and contractility of actin filaments (De La Cruz and Ostap 2004; Vicente-Manzanares et al. 2009). These contractile proteins are found in cardiac, skeletal and smooth muscle, in which sliding crossbridges that connect thick myosin filaments with thin actin filaments provide the force needed.

Non-muscle myosin type IIA is the molecular motor also in myofibroblasts (Lecarpentier et al. 2021) and would explain the stronger expression of S100A4 in actin positive myofibroblasts compared to fibroblasts.

Alternatively, S100A4 positivity seen in CD4 + and CD8 + positive T cells does not seem to be essential for cell motility/migration and inflammatory potential (Weatherly et al. 2015). S100A4 protein in these cells seems to play a role in T-cell lineage differentiation, altering the expression of transcription factors and signal transduction pathway genes (Weatherly et al. 2015).

Other regulatory and adaptive functions are linked to S100A4 positivity in the kidney. Researchers have shown that the absence of S100A4 profoundly delayed osmoadaptation and slowed cellular growth under hypertonic conditions (Rivard et al. 2007). S100A4 also appears to have an important function in the adipocyte metabolism. It was shown that S100A4 is an inhibitory factor for obesity and attenuates the inflammatory reaction, while activating the Akt signalling pathway (Hou et al. 2018).

Based on our observations, S100A4 is expressed in a broad spectrum of cells with different functions in different locations and is not specifically (if at all) found in fibroblasts. It is therefore not possible to link the expression of this protein to fibroblasts and therefore transition from epithelia to fibroblasts as done in published data (Zeisberg et al. 2007; Strutz et al. 1995). Accordingly, some research groups have been unable to prove any evidence of epithelial mesenchymal transition. A paper published by Kriz et al (Koesters et al. 2010) used a transgenic mouse model to induce TGF-beta1 in tubular epithelial cells after tetracycline application. TGF-beta1 has been proposed as a crucial factor to complete EMT (Gao et al. 2015). The above investigators found that diffuse fibrosis is observed in the kidney already at day 2 after TGF-beta1 induction, preceding any tubular damage. Further they could show that resident fibroblasts in the peritubular spaces proliferate (Ki-67 positive) and that myofibroblasts develop from resident fibroblasts. These observations were confirmed by Le Hir et al (Picard et al. 2008). Resident peritubular fibroblasts proliferated and showed progressive alterations, suggesting a transformation into myofibroblasts, which are said to be responsible for the increased production of intercellular matrix and fibrosis, eventually leading to chronic renal failure. Additionally, tracing of tubular profiles (TEM) did not reveal gaps or defects in the tubular basement membrane and no cells were observed to cross the tubular basement membrane. The tubular cells accumulated lysosomal elements throughout the cell at day 4

after TGF-beta1 induction (begin of autophagic process) but no positivity for S100A4 was observed in the tubules during the investigated time course. These findings suggest that upon damage, inflammatory cells migrate to the kidney, many of which express S100A4. Local fibroblasts proliferate and some transform to myofibroblasts that lead to fibrosis and depending on the severity and chronicity of the damage, to chronic renal failure.

After reappraising the originally published images during the emergence of the EMT type 2 theory (Strutz et al. 1995; Zeisberg et al. 2007), it is striking that the histological images depicted mostly show a nuclear S100A4 positivity in round cells with oval to kidney-bean shaped nuclei. This morphology is more consistent with monocytes/macrophages than spindle shaped fibroblasts/myofibroblasts, which have an elongated and flattened nucleus. Also, our immunohistochemical evaluations mainly show a cytoplasmic rather than a nuclear positivity in fibroblasts/myofibroblast.

In addition, under normal circumstances, S100A4 is expressed by many epithelial segments of the kidney without the epithelia being in an epithelial-mesenchymal transition. Therefore, an epithelial positivity for S100A4 cannot be equated to mesenchymal transition.

Taken together, the evidence for type 2 EMT is not very compelling. The S100A4 antibody labels many cells of the immune system, occasional epithelial cells as well as some fibroblasts/myofibroblasts. In the setting of chronic inflammation, as used in the original description of EMT type 2, a separation of inflammatory cells from fibroblast based on S100A4 positivity is therefore not possible. The insights gained by employing S100A4 to prove EMT type 2 consequently need to be interpreted with caution.

Declarations

The authors have no relevant financial or non-financial interests to disclose.

Compliance with ethical standards

The authors state that they comply with the ethical standards specified by Histochemistry Cell Biology. The study was approved by the Ethics Committee Northwestern and Central Switzerland (EKNZ).

Funding

No funding was received for conducting this study.

Conflict of interest

The authors declare no conflict of interest.

Contributions

All authors contributed to the study conception and design. B.MF collected, analyzed and interpreted data, wrote the manuscript; A.H and M.B. collected data and critically reviewed the manuscript; E.C-R and

C.O: collected, analyzed and interpreted data, and critically reviewed the manuscript; A.V: conceived and designed the project, collected, analyzed and interpreted data, wrote the manuscript and gave final approval. All authors read and approved the final manuscript.

References

1. Burns WC, Thomas MC (2010) The molecular mediators of type 2 epithelial to mesenchymal transition (EMT) and their role in renal pathophysiology. Expert reviews in molecular medicine 12:e17. doi:10.1017/s1462399410001481
2. De La Cruz EM, Ostap EM (2004) Relating biochemistry and function in the myosin superfamily. Current opinion in cell biology 16 (1):61–67. doi:10.1016/j.ceb.2003.11.011
3. Fei F, Qu J, Li C, Wang X, Li Y, Zhang S (2017) Role of metastasis-induced protein S100A4 in human non-tumor pathophysiologies. Cell & bioscience 7:64. doi:10.1186/s13578-017-0191-1
4. Gao J, Yan Q, Wang J, Liu S, Yang X (2015) Epithelial-to-mesenchymal transition induced by TGF-β1 is mediated by AP1-dependent EpCAM expression in MCF-7 cells. Journal of cellular physiology 230 (4):775–782. doi:10.1002/jcp.24802
5. Garrett SC, Hodgson L, Rybin A, Toutchkine A, Hahn KM, Lawrence DS, Bresnick AR (2008) A biosensor of S100A4 metastasis factor activation: inhibitor screening and cellular activation dynamics. Biochemistry 47 (3):986–996. doi:10.1021/bi7021624
6. Gonzalez-Martinez T, Perez-Piñera P, Díaz-Esnal B, Vega JA (2003) S-100 proteins in the human peripheral nervous system. Microscopy research and technique 60 (6):633–638. doi:10.1002/jemt.10304
7. Hou S, Jiao Y, Yuan Q, Zhai J, Tian T, Sun K, Chen Z, Wu Z, Zhang J (2018) S100A4 protects mice from high-fat diet-induced obesity and inflammation. Laboratory investigation; a journal of technical methods and pathology 98 (8):1025–1038. doi:10.1038/s41374-018-0067-y
8. Jenkinson SR, Barraclough R, West CR, Rudland PS (2004) S100A4 regulates cell motility and invasion in an in vitro model for breast cancer metastasis. British journal of cancer 90 (1):253–262. doi:10.1038/sj.bjc.6601483
9. Kalluri R, Weinberg RA (2009) The basics of epithelial-mesenchymal transition. The Journal of clinical investigation 119 (6):1420–1428. doi:10.1172/jci39104
10. Kiener HP, Watts GF, Cui Y, Wright J, Thornhill TS, Sköld M, Behar SM, Niederreiter B, Lu J, Cernadas M, Coyle AJ, Sims GP, Smolen J, Warman ML, Brenner MB, Lee DM (2010) Synovial fibroblasts self-direct multicellular lining architecture and synthetic function in three-dimensional organ culture. Arthritis and rheumatism 62 (3):742–752. doi:10.1002/art.27285
11. Kim EJ, Helfman DM (2003) Characterization of the metastasis-associated protein, S100A4. Roles of calcium binding and dimerization in cellular localization and interaction with myosin. The Journal of biological chemistry 278 (32):30063–30073. doi:10.1074/jbc.M304909200

12. Koesters R, Kaissling B, Lehir M, Picard N, Theilig F, Gebhardt R, Glick AB, Hähnel B, Hosser H, Gröne HJ, Kriz W (2010) Tubular overexpression of transforming growth factor-beta1 induces autophagy and fibrosis but not mesenchymal transition of renal epithelial cells. The American journal of pathology 177 (2):632–643. doi:10.2353/ajpath.2010.091012
13. Kriajevska M, Fischer-Larsen M, Moertz E, Vorm O, Tulchinsky E, Grigorian M, Ambartsumian N, Lukanidin E (2002) Liprin beta 1, a member of the family of LAR transmembrane tyrosine phosphatase-interacting proteins, is a new target for the metastasis-associated protein S100A4 (Mts1). The Journal of biological chemistry 277 (7):5229–5235. doi:10.1074/jbc.M110976200
14. Kriajevska MV, Cardenas MN, Grigorian MS, Ambartsumian NS, Georgiev GP, Lukanidin EM (1994) Non-muscle myosin heavy chain as a possible target for protein encoded by metastasis-related mts-1 gene. The Journal of biological chemistry 269 (31):19679–19682
15. Lecarpentier Y, Claes V, Hébert JL, Schussler O, Vallée A (2021) Mechanical and Thermodynamic Properties of Non-Muscle Contractile Tissues: The Myofibroblast and the Molecular Motor Non-Muscle Myosin Type IIA. International journal of molecular sciences 22 (14). doi:10.3390/ijms22147738
16. Li ZH, Bresnick AR (2006) The S100A4 metastasis factor regulates cellular motility via a direct interaction with myosin-IIA. Cancer research 66 (10):5173–5180. doi:10.1158/0008-5472.can-05-3087
17. Li ZH, Dulyaninova NG, House RP, Almo SC, Bresnick AR (2010) S100A4 regulates macrophage chemotaxis. Molecular biology of the cell 21 (15):2598–2610. doi:10.1091/mbc.e09-07-0609
18. Picard N, Baum O, Vogetseder A, Kaissling B, Le Hir M (2008) Origin of renal myofibroblasts in the model of unilateral ureter obstruction in the rat. Histochemistry and cell biology 130 (1):141–155. doi:10.1007/s00418-008-0433-8
19. Ramagopal UA, Dulyaninova NG, Varney KM, Wilder PT, Nallamsetty S, Brenowitz M, Weber DJ, Almo SC, Bresnick AR (2013) Structure of the S100A4/myosin-IIA complex. BMC structural biology 13:31. doi:10.1186/1472-6807-13-31
20. Rivard CJ, Brown LM, Almeida NE, Maunsbach AB, Pihakaski-Maunsbach K, Andres-Hernando A, Capasso JM, Berl T (2007) Expression of the calcium-binding protein S100A4 is markedly up-regulated by osmotic stress and is involved in the renal osmoadaptive response. The Journal of biological chemistry 282 (9):6644–6652. doi:10.1074/jbc.M609432200
21. Saitoh M (2018) Involvement of partial EMT in cancer progression. Journal of biochemistry 164 (4):257–264. doi:10.1093/jb/mvy047
22. Sherbet GV (2009) Metastasis promoter S100A4 is a potentially valuable molecular target for cancer therapy. Cancer letters 280 (1):15–30. doi:10.1016/j.canlet.2008.10.037
23. Sherbet GV, Lakshmi MS (1998) S100A4 (MTS1) calcium binding protein in cancer growth, invasion and metastasis. Anticancer research 18 (4a):2415–2421
24. Strutz F, Okada H, Lo CW, Danoff T, Carone RL, Tomaszewski JE, Neilson EG (1995) Identification and characterization of a fibroblast marker: FSP1. The Journal of cell biology 130 (2):393–405.

doi:10.1083/jcb.130.2.393

25. Takenaga K, Nakamura Y, Sakiyama S, Hasegawa Y, Sato K, Endo H (1994) Binding of pEL98 protein, an S100-related calcium-binding protein, to nonmuscle tropomyosin. The Journal of cell biology 124 (5):757–768. doi:10.1083/jcb.124.5.757
26. Thiery JP, Acloque H, Huang RY, Nieto MA (2009) Epithelial-mesenchymal transitions in development and disease. Cell 139 (5):871–890. doi:10.1016/j.cell.2009.11.007
27. Vicente-Manzanares M, Ma X, Adelstein RS, Horwitz AR (2009) Non-muscle myosin II takes centre stage in cell adhesion and migration. Nature reviews Molecular cell biology 10 (11):778–790. doi:10.1038/nrm2786
28. Wang Y, Ding SJ, Wang W, Jacobs JM, Qian WJ, Moore RJ, Yang F, Camp DG, 2nd, Smith RD, Klemke RL (2007) Profiling signaling polarity in chemotactic cells. Proceedings of the National Academy of Sciences of the United States of America 104 (20):8328–8333. doi:10.1073/pnas.0701103104
29. Weatherly K, Bettonville M, Torres D, Kohler A, Goriely S, Braun MY (2015) Functional profile of S100A4-deficient T cells. Immunity, inflammation and disease 3 (4):431–444. doi:10.1002/iid3.85
30. Zeisberg M, Yang C, Martino M, Duncan MB, Rieder F, Tanjore H, Kalluri R (2007) Fibroblasts derive from hepatocytes in liver fibrosis via epithelial to mesenchymal transition. The Journal of biological chemistry 282 (32):23337–23347. doi:10.1074/jbc.M700194200

Figures

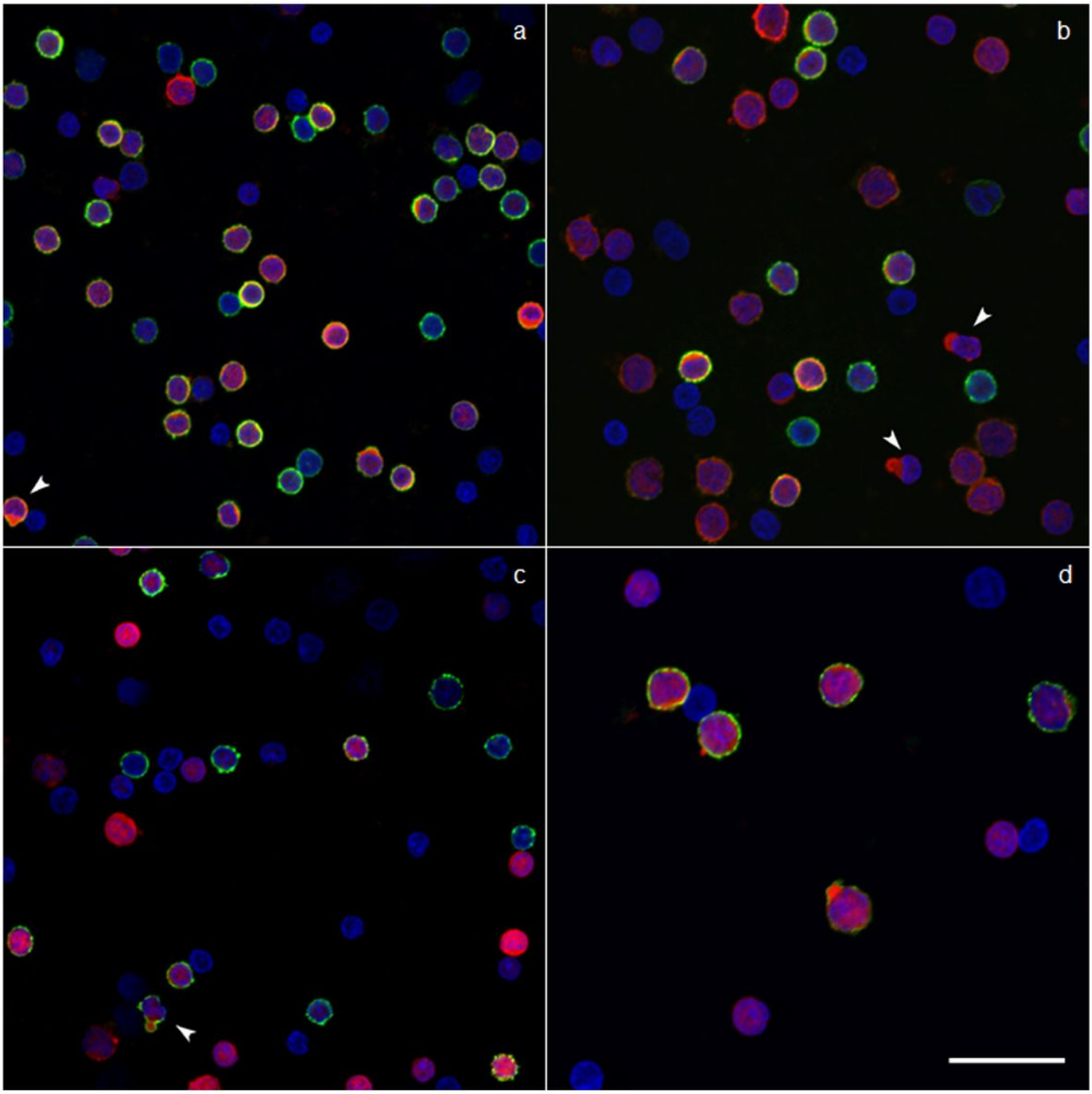

Figure 1

Isolated leukocytes co-stained with various leucocyte markers and FSP1/S100A4, then visualized by immunofluorescence (IF) staining. a: Co-staining of CD3 (green) and S100A4 (red), magnification 500x. b: Co-staining of CD4 (green) and S100A4 (red), (500x). c: Co-staining of CD8 (green) and S100A4 (red), (550x). d: Co-staining of CD14 (green) and FSP1/S100A4 (red), (600x). DAPI stain (blue). Arrowheads: mature cytotoxic T-cells. Scale bar 40 μm

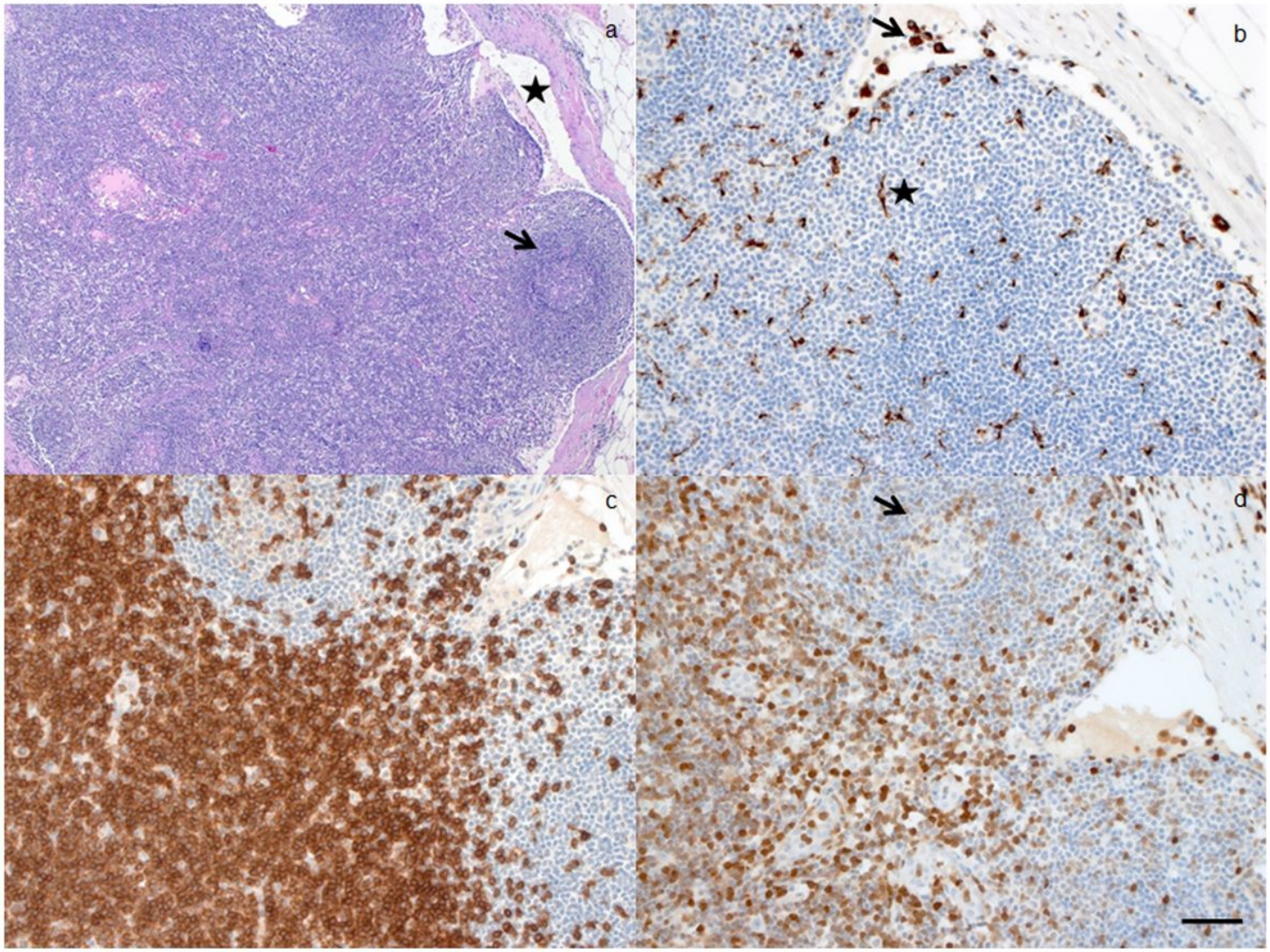

Figure 2

a: Lymph node showing a secondary lymph follicle (arrow), predominantly composed of B lymphocytes, adjacent to the subcapsular sinus (star); Hematoxylin and eosin stain, magnification 50x. b: CD68 immunohistochemical staining, positive in dendritic cells (star) and other histiocytes like sinus histiocytes (arrow), (200×). c: CD3 immunohistochemical staining, positive in CD4+ and CD8+ T-lymphocytes, (200x). d: S100A4 staining, predominantly positive in the T-cell rich paracortex and predominantly negative in the B-cell rich secondary lymph follicle (arrow), (200x). Scale bar 100 μm

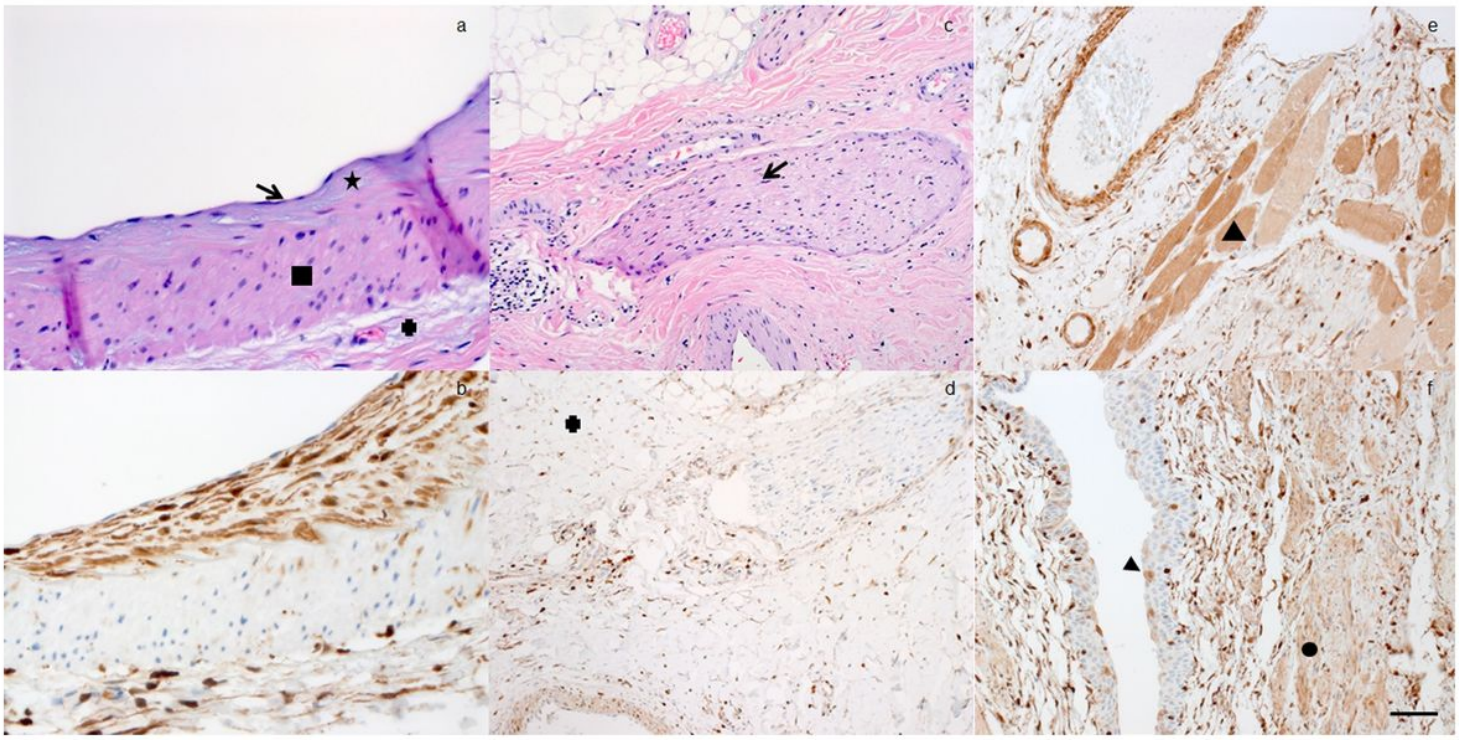

Figure 3

a: Section of an arterial vessel with endothelium (arrow), subendothelial space (star), tunica media (square) and tunica adventitia (cross); Hematoxylin and eosin stain, magnification 400x. b: S100A4 staining most of the cells of the subendothelial space, made up of intimal smooth muscle cells and stellate-shaped pericyte-like cells. Some positive cells are seen in the tunica media composed of smooth muscle cells and in the loose connective tissue of the tunica adventitia, (400x). c: Connective tissue showing a peripheral nerve (arrow) and blood vessels adjacent to adipocytes (cross); Hematoxylin and eosin stain (200×). d: S100A4 staining positive in some adipocytes (cross) and negative in a peripheral nerve (arrow), (200x). e: Skeletal muscle (triangle) with S100A4 positivity (200x). f: Urothelial mucosa showing some S100A4 positive umbrella cells (arrowhead) with adjacent smooth muscle layer (circle) with positivity for S100A4 (200x). Scale bar 100 μm

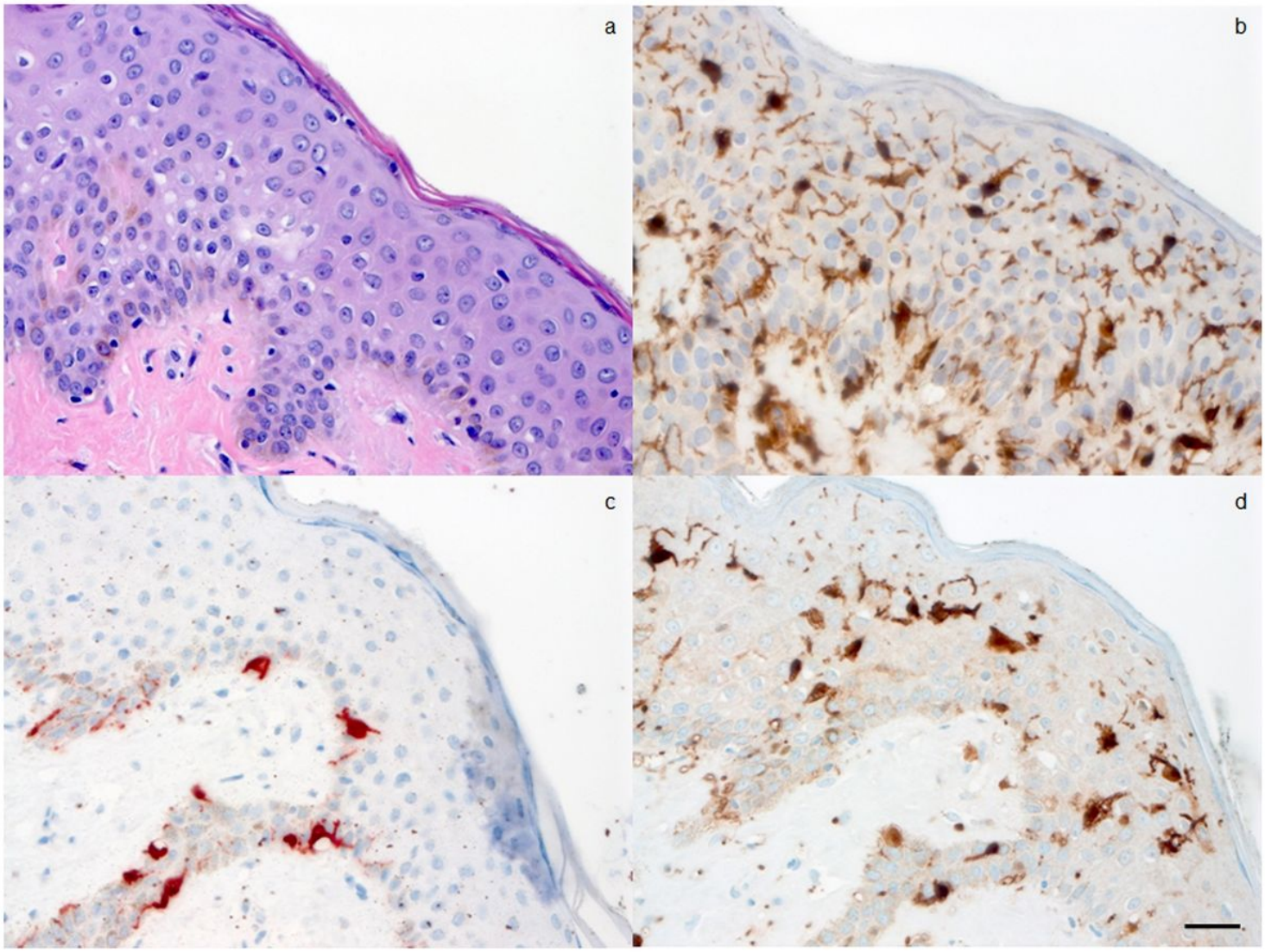

Figure 4

a: Skin with slightly pigmented epidermis; hematoxylin and eosin stain, magnification 400x. b: S100A4 staining mainly Langerhans histiocytes (400x). c: MART-1/Tyrosinase staining melanocytes of the epidermis, negative in Langerhans cells (400x). d: S100 (Dako Omnis) reacts strongly with human S100B and is positive in Langerhans cells (400x). Scale bar 50 µm

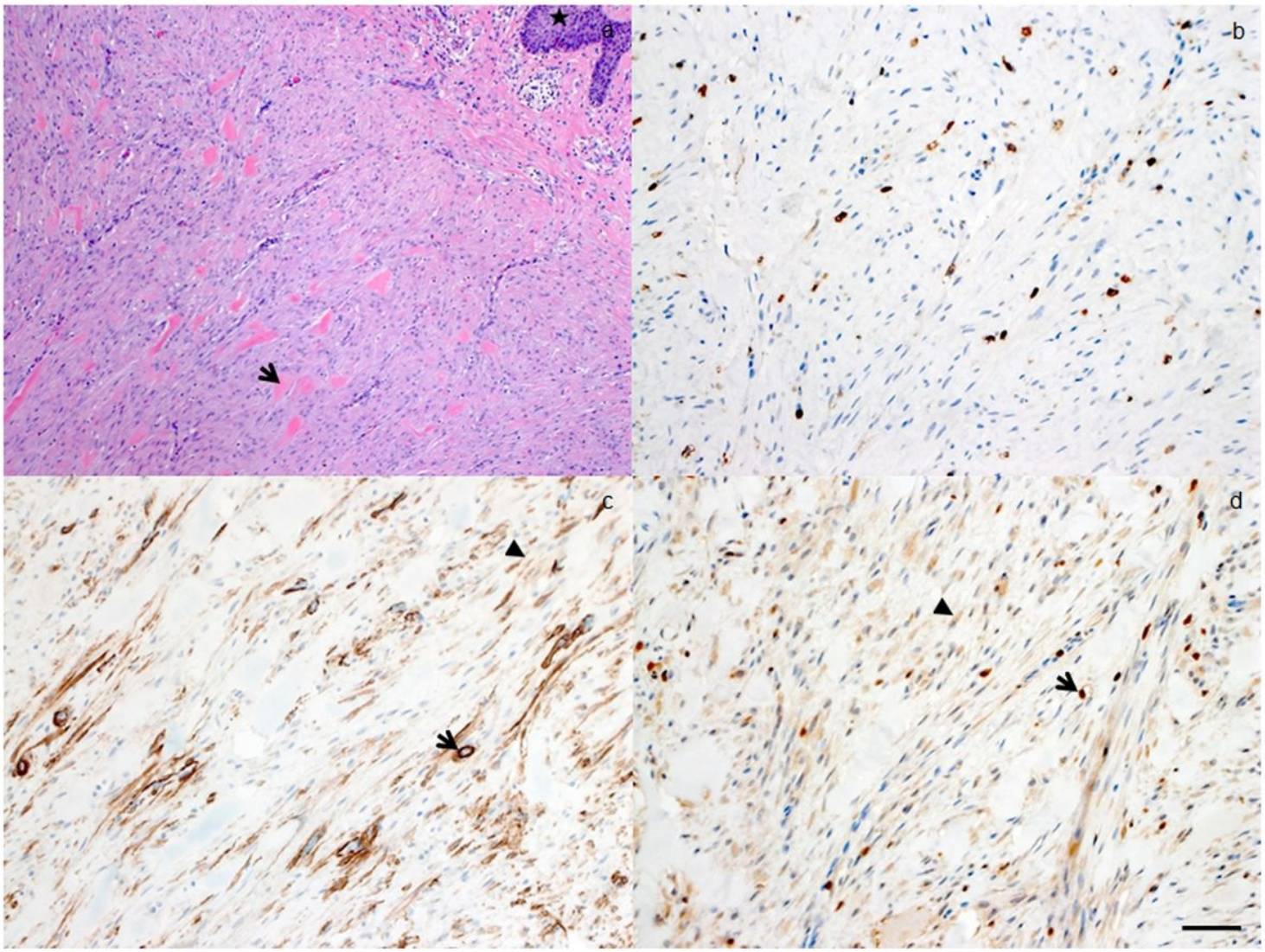

Figure 5

a: Hypertrophic scar tissue in the dermis of the skin with focal epidermis (star), composed of fibroblasts/myofibroblasts (arrowhead), mononuclear inflammatory cell and keloid like fibrosis (arrow); hematoxylin and eosin stain, magnification 100x. b: CD45 immunohistochemical staining (expressed in most leucocytes) highlighting the inflammatory cells in the scar tissue (200x). c: Immunohistochemical staining for actin; expressed in myofibroblasts (arrowhead) and small blood vessels (arrow) (200x). d: S100A4 expressed in the cytoplasm of some fibroblasts/myofibroblasts (arrowhead). Strong nuclear and cytoplasmic expression in resident inflammatory cells and small blood vessels (arrow) (200x). Scale bar 100 µm

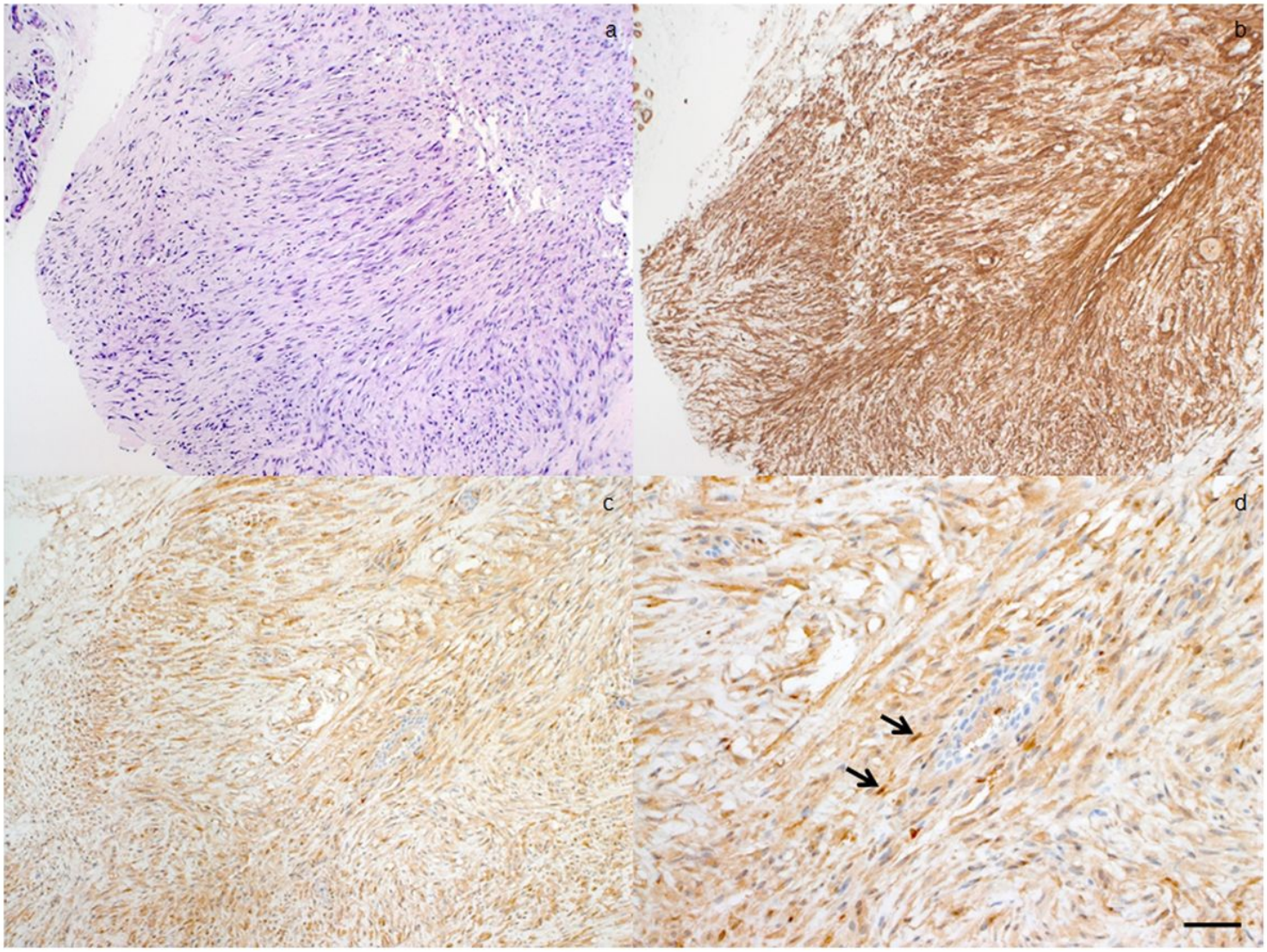

Figure 6

a: Nodular proliferation of predominantly myofibroblasts in Dupuytren's contracture (Palmar Fibromatosis); Hematoxylin and eosin stain, magnification 100x. b: Immunohistochemical staining for smooth muscle actin highlighting the predominant population of myofibroblasts (100x). c: A moderate expression of S100A4 in the cytoplasm of most myofibroblasts (100x). d: S100A4 staining at higher magnification (200x) also shows some vessel associated positive cells (arrows). Scale bar 100 μm

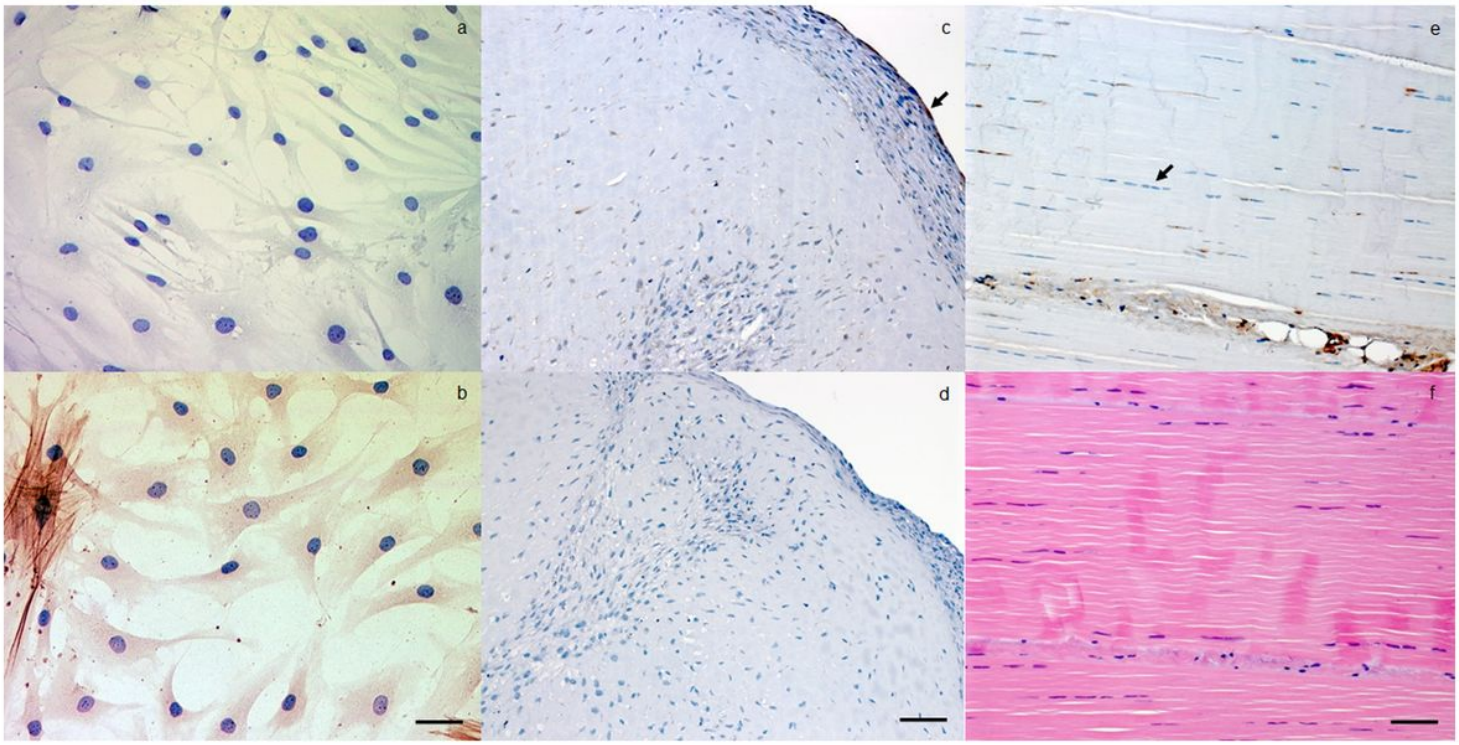

Figure 7

a: Cultured synovial fibroblasts are predominantly negative for S100A4, magnification 630x. b: Smooth muscle actin positive in a few myofibroblasts (630x). c: 3D cultured synovial fibroblasts are predominantly negative for S100A4 with some positive cells in the perimeter (arrow) (200x). d: 3D cultured synovial fibroblasts negative for smooth muscle actin (200x). e: Tendon fibroblasts (arrow) are predominantly negative for S100A4. f: Hematoxylin and eosin stain of a tendon (200x). Scale bar 100 μm

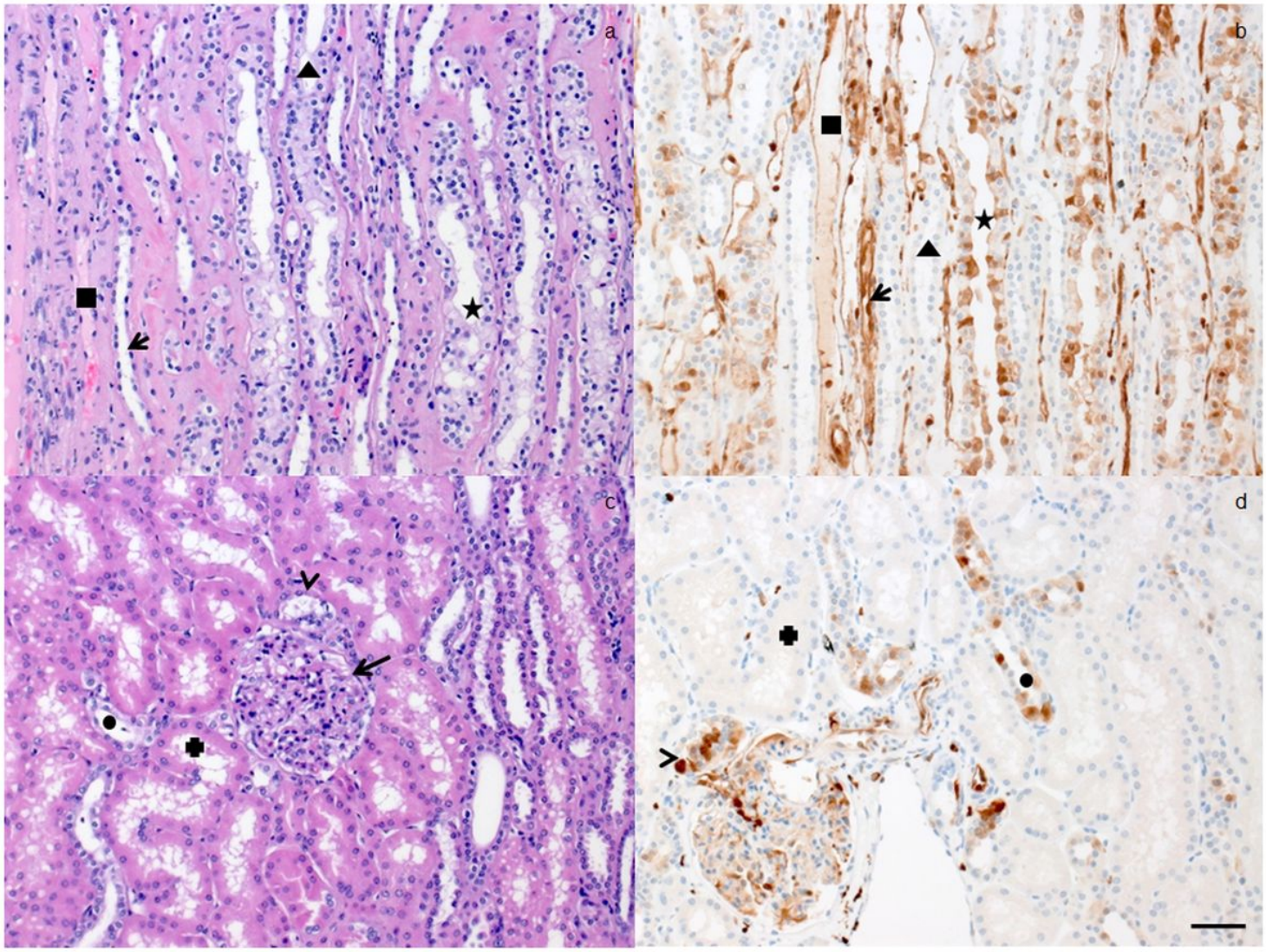

Figure 8

a: Renal medulla made up of vasa rectae renis (square), collecting ducts (star), distal tubules (triangle) and loop of Henle (arrow), magnification 200x. b: S100A4 staining of the renal medulla highlighting some positive cells (cytoplasmic and nuclear) in the collecting ducts (star), loop of Henle (arrow) and vasculature (square). Most of the cells in the distal tubules are negative (triangle) (200x). c: Renal cortex with a glomerulus (arrow), macula densa (arrowhead), proximal tubules (cross) and some distal tubules (circle) (200x). d: S100A4 staining of the cortex with positivity in some cells of the distal tubules (circle), pronounced in the macula densa (arrowhead). The proximal tubules are negative for S100A4 (cross) (200x). Scale bar 100 µm